

Shape of optimal active flagella

Eric Lauga¹ and Christophe Eloy^{1,2}

¹Department of Mechanical and Aerospace Engineering, University of California San Diego,
9500 Gilman Drive, La Jolla CA 92093-0411, USA;

²Aix-Marseille University, IRPHE UMR 7342, CNRS, Marseille, France.

(Received 6 February 2022)

Many eukaryotic cells use the active waving motion of flexible flagella to self-propel in viscous fluids. However, the criteria governing the selection of particular flagellar waveforms among all possible shapes has proved elusive so far. To address this question, we derive computationally the optimal shape of an internally-forced periodic planar flagellum deforming as a travelling wave. The optimum is here defined as the shape leading to a given swimming speed with minimum energetic cost. To calculate the energetic cost though, we consider the irreversible internal power expended by the molecular motors forcing the flagellum, only a portion of which ending up dissipated in the fluid. This optimisation approach allows us to derive a family of shapes depending on a single dimensionless number quantifying the relative importance of elastic to viscous effects: the *Sperm* number. The computed optimal shapes are found to agree with the waveforms observed on spermatozoon of marine organisms, thus suggesting that these eukaryotic flagella might have evolved to be mechanically optimal.

1. Introduction

Many microorganisms swimming in viscous fluids actuate slender appendages, be they flagella or cilia, in a wavelike fashion in order to propel themselves (Brennen & Winnet 1977; Lighthill 1975; Childress 1981; Lauga & Powers 2009). The origin of this waving motion rests in the mechanical properties of the surrounding fluid at low Reynolds number. In the absence of inertia, the Stokes equations are time-reversible and thus any time-reversible deformation of a swimmer or its appendages would result in no average locomotion (Purcell 1977). To bypass this constraint, microorganisms swim, in general, by using the simplest deformation kinematics indicating a clear direction of time: the travelling wave (Lauga 2011).

As we are all too aware from our efforts at the pool, being able to swim does not however mean one does it efficiently. In the context of cell motility, a question that has received some attention in the literature is the issue of optimal low-Reynolds number locomotion. With infinite degrees of freedom in shape, design, and actuation mechanism, what is the most effective way to self-propel in the absence of inertia? Since the locomotion kinematics in the Stokesian regime scales linearly with the typical actuation frequency of the body, a swimming efficiency needs first to be defined to normalise the swimming speed and make the optimality criterion frequency-independent (Lighthill 1975). This is typically done by comparing the work done against the fluid to swim (total power) to the work that would be expended by a force dragging the same swimmer at the same speed (useful power). Optimal swimming is then equivalent to either swimming at a fixed speed with minimum power or swimming at fixed power with maximum speed.

For some swimmers amenable to precise mathematical or numerical analysis, calculations of optimal kinematics have been proposed. For instance, the optimal swimming

gait of a Purcell's three-link swimmer (Purcell 1977) has been characterised by Tam & Hosoi (2007) and Avron & Raz (2008), as well as the optimal kinematics of the related three-sphere swimmer (Alouges *et al.* 2008). Shapere & Wilczek (1987, 1989*a,b*) showed analytically that the optimal swimming by surface deformation of spheres and cylinders is achieved by surface waves akin to metachronal waves observed in ciliary fluid transport (Brennen & Winnet 1977), for which the optimal kinematics has also been studied (e.g. Osterman & Vilfan 2011). For swimmers able to impose a tangential velocity on the fluid at their surface without deforming their shapes, a swimming motion referred to as squirming, infinite efficiency can be obtained for infinitely slender swimmers as shown by Leshansky *et al.* (2007). For a spherical squirmer however, the optimal large-amplitude swimming (Michelin & Lauga 2010) or feeding (Michelin & Lauga 2011, 2013) problem has a finite efficiency and displays, again, surface waves.

Unfortunately, most microorganisms do not have shapes allowing detailed mathematical derivations. The most common shape is that of a cell body, somewhat spheroidal in shape, attached to one or several flagella (Bray 2000). Eukaryotic cells have active internally-forced flagella forming planar waves, while bacteria rotate passive helical flagella. The presence of slender flagella allows, physically, microorganisms to take full advantage of drag anisotropy at low Reynolds number in order to generate drag-based thrust (Lauga & Powers 2009). In the context of this flagellar swimming, once the issue of optimal body-to-flagella size has been addressed (Higdon 1979*a,b*; Fujita & Kawai 2001), the important question becomes how to actuate a flagellum optimally?

For bacteria locomotion, the optimal shape of rotated rigid helical flagella was recently derived and found to agree with experimental observations (Spagnolie & Lauga 2011). For eukaryotic cells however, the optimal flagellar shape has to be different from the bacterial one since flagella are deformed actively. A pioneering study demonstrated that, for a given flagellar shape, the optimal instantaneous shape deformation is that of a travelling wave (Pironneau & Katz 1974). Using a local analysis for the fluid dynamics, Lighthill then derived the optimal shape for a flagellar travelling wave. For an infinite swimmer, he obtained a sawtooth wave (Lighthill 1975), an optimal which remains valid for finite-size swimmers (Pironneau & Katz 1974, 1975).

The optimal flagellar shape thus appears to be mathematically singular. Yet experimental observations do not show any singularity (Brennen & Winnet 1977). To resolve the discrepancy, different possibilities can be considered. A first possibility could be that the shapes of eukaryotic flagella have not evolved to be optimal for locomotion, either because locomotion contributes to relatively small energetic costs, or because other contributions are more relevant biologically. Another possibility could be that cells cannot reach the mathematical optimum because of physical, biochemical, or mechanical constraints. A last possibility could resolve the apparent discrepancy: flagella might well be optimal but the energetic costs measured through the power lost in the fluid might not be the pertinent one. The internal structure of an eukaryotic flagellum, called the axoneme, is made up of a small number of polymeric filaments (microtubule doublets) which are caused to slide past each other by the action of a motor protein called the dynein (Alberts *et al.* 2007). It is the action of these molecular motors on the filaments that performs useful work through the consumption of ATP. Only a fraction of this work ends up dissipated in the fluid however, the other fraction being spent on irreversible bending of the flagellum. Because it quantifies the real biological cost of actuating the flagellum, the work done by these molecular motor is the correct energetic measure and we believe that efficiency should be defined on this measure to perform adequate optimisation calculations (Eloy & Lauga 2012).

In this paper we use this internal energetic measure to derive the shape of the optimal

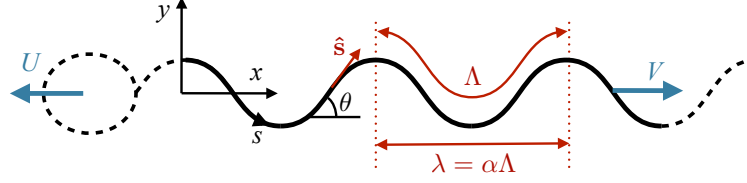


FIGURE 1. Mathematical model and notation. We consider an infinite planar flagellum of wavelength λ along x , with curvilinear coordinate s and tangent unit vectors $\hat{\mathbf{s}}$. The wavespeed is denoted V in the $+x$ direction and the flagellum is assumed to be swimming with speed $-U$. The wavelength measured along the curvilinear direction is $\Lambda \equiv \lambda/\alpha$ ($\alpha \leq 1$).

active flagellum. After introducing the physical model for an active, internally-forced periodic planar flagellum in §2, we compute the travelling-wave shape that maximises the swimming speed for a fixed energetic cost in §3. The shape is a function of a dimensionless Sperm number, Sp , quantifying the relative importance of bending to viscous forces. For finite values of Sp , the optimal flagellar waveform is smooth and becomes singular only in the hydrodynamic limit, $\text{Sp} \rightarrow \infty$. In the elastic limit $\text{Sp} \rightarrow 0$, the optimal waveform is composed of circular arcs with constant curvature of alternating signs. Our optimal shapes are found to agree with experimentally-measured waveforms of marine microorganisms as discussed in §4.

2. Mathematical model of active flagellum

2.1. Kinematics

We consider an infinite, active, and flexible planar flagellum deforming periodically such that it swims at constant velocity $-U$ in the x -direction (figure 1). The flagellum deformation is assumed to be a travelling wave of velocity V and wavelength λ along x (or, equivalently, Λ along the curvilinear coordinate s , with $\lambda = \alpha\Lambda$, $\alpha \leq 1$). The local tangential unit vector is defined as $\hat{\mathbf{s}}$.

In the frame moving with velocity $V - U$ compared to the laboratory frame, the deformation of the flagellum appears steady (Lighthill 1975). In this frame, the material points on the flagellum move thus necessarily tangentially with velocity $-c\hat{\mathbf{s}}$, where the speed c is such that a material point travels one wavelength Λ over a period T . Consequently, we have $T = \Lambda/c = \lambda/V$ and thus $V = \alpha c$, where

$$\alpha = \frac{\lambda}{\Lambda} = \frac{1}{\Lambda} \int_0^\Lambda \cos \theta \, ds, \quad (2.1)$$

and θ is the local angle between the flagellum and the swimming direction (figure 1). The relative velocity between the fluid and the flagellum is therefore given, at any point along the flagellum, by

$$\mathbf{u} = (V - U)\hat{\mathbf{x}} - c\hat{\mathbf{s}}, \quad (2.2)$$

with a spatial dependence coming implicitly through the variation of $\hat{\mathbf{s}}$.

2.2. Swimming

In order to compute the fluid forces on the waving flagellum, we use the classical framework of resistive force theory (Gray & Hancock 1955), which is the leading-order term of slender-body theory (Cox 1970). Within this approximation, the force per unit length exerted by the fluid on the flagellum can be written as

$$\mathbf{F} = \xi_\perp \mathbf{u} + (\xi_\parallel - \xi_\perp) \hat{\mathbf{s}} \hat{\mathbf{s}} \cdot \mathbf{u}, \quad (2.3)$$

where ξ_{\perp} and ξ_{\parallel} are the perpendicular and parallel resistance coefficients respectively, and we will further assume that $\xi_{\perp} = 2\xi_{\parallel}$. Inserting (2.2) into (2.3) yields a spatial distribution of force such that

$$\frac{1}{\xi_{\perp}} \mathbf{F} \cdot \hat{\mathbf{x}} = (\alpha c - U)(1 - \frac{1}{2} \cos^2 \theta) - \frac{1}{2} c \cos \theta. \quad (2.4)$$

To determine U , we enforce that the net sum of all hydrodynamic forces projected along the x -direction is zero (free-swimming condition), i.e. $\int_0^{\Lambda} \mathbf{F} \cdot \hat{\mathbf{x}} \, ds = 0$ (Lighthill 1975), leading to the swimming velocity U given by

$$U = \frac{1 - \beta}{2 - \beta} \alpha c, \quad \text{with } \beta = \frac{1}{\Lambda} \int_0^{\Lambda} \cos^2 \theta \, ds. \quad (2.5)$$

Note that since $c > 0$ and $\beta \leq 1$, then $U \geq 0$: a wave travelling to the right leads to swimming to the left.

2.3. Energetics

In order to evaluate the power needed to deform periodically the flagellum, we first need to calculate the active internal torques necessary to the deformation. We use Kirchhoff equations for a flexible rod (Audoly & Pomeau 2010) expressing the local balance of forces and moments. In that case, the internal tension, \mathbf{T} , and bending moment, \mathbf{M} , are related to the external force according to

$$\mathbf{T}' = \mathbf{F}, \quad \mathbf{M}' + \hat{\mathbf{s}} \times \mathbf{T} + \mathbf{q} = 0, \quad (2.6)$$

where primes denote differentiation with respect to the local curvilinear direction s , and \mathbf{q} denotes the active torque produced by the internal molecular motors. Assuming a Hookean constitutive relation, $\mathbf{M} = B\theta''\hat{\mathbf{z}}$, where B is the bending rigidity, the equations (2.6) yields an explicit expression for the internal torque as

$$\mathbf{q} = -B\theta''\hat{\mathbf{z}} + \hat{\mathbf{s}} \times \int_s^L \mathbf{F} \, ds, \quad (2.7)$$

where L denotes the end of the flagellum or any point with the same phase (in practice any point can be chosen for L since a s -shift is equivalent to a time shift).

The average power needed to perform the deformation is obtained from the scalar product of the internal torque and the local angular velocity

$$P = \int_0^{\Lambda} [\mathbf{q} \cdot \dot{\theta}\hat{\mathbf{z}}]^+ \, ds, \quad (2.8)$$

where $\dot{\theta} = -c\theta'$ is the angular velocity and the notation $[\cdot]^+$ expresses that only positive works are included in the energy budget. In other words, we assume that the flagellum (or more precisely, the molecular motors actuating it) cannot harvest energy from the fluid when the local power given to the fluid is negative. This means that the elastic energy is not conserved and that the work expended by internal torques is not totally transferred to the fluid, but instead a portion of it is wasted internally due to the irreversibility of internal motors. This assumption is similar to what is classically done when modelling the muscle mechanics, except that, in the present study, the work is done in bending instead of longitudinal compression or extension (Alexander 1992).

2.4. Swimming efficiency

The efficiency, η , of a given flagellum deformation, $\theta(s)$, is then expressed as the ratio between the power needed to drag one period of the straightened filament in the fluid to

the actual power spent to actuate the internal motors

$$\eta = \frac{\xi_{\parallel} \Lambda U^2}{P}. \quad (2.9)$$

This efficiency depends on a single dimensionless parameter, the Sperm number Sp , defined as

$$\text{Sp} = \frac{\Lambda}{\ell}, \quad \text{with } \ell = \left(\frac{TB}{\xi_{\perp}} \right)^{1/4} \quad (2.10)$$

which measures the ratio of the wavelength, Λ , to an elasto-viscous persistence length, ℓ . In the traditional approach for optimisation of locomotion at low Reynolds number, the efficiency, denoted η_{fluid} here, is defined as in (2.9) but P is taken to be the rate of energy dissipated in the fluid, and the elastic nature of the flagellum is not considered (Lauga & Powers 2009). This was the assumption made by Lighthill in his optimisation calculation (Lighthill 1975). With P defined as in (2.8), the optimisation approach proposed allows us to rigorously quantify the net molecular energy expenditure. As a result, the optimal shape is a function of the elastic modulus of the flagellum through the Sperm number.

3. Shape of the optimal active flagellum

3.1. Numerical optimisation

The optimisation procedure consists in computing, for a given Sperm number Sp , the flagellum shape that maximises the efficiency. This optimisation problem can be solved numerically by decomposing the flagellum shape onto Fourier modes, such that the local angle is given by $\theta(s - ct) = \sum_{n=1}^N A_n \cos[2\pi n(s - ct)/\Lambda]$, where, in fact, even terms are zero for the optimal shapes due to the problem symmetry. The swimming velocity can then be determined using (2.5), and the efficiency using (2.9). From a practical point of view, the Fourier series has been truncated with $N = 100$ to have a sufficient spectral resolution, and integrals along s have been discretized onto 1000 elements. The optimisation itself is carried out with MATLAB using the sequential programming (SQP) algorithm, starting from a guess value picked as the best efficiency among 1000 random trials. The optimisation calculation is typically ran 20 times for each Sperm number to ensure that the algorithm has reached the global optimum. This approach has been validated by comparing the results for large values of Sp with the analytical study of Lighthill (1975). He found that, in the hydrodynamic limit where all the work is dissipated in the fluid (equivalent to vanishing bending rigidity, or infinite Sp), the maximum efficiency $\eta_{\text{fluid}} = (1 - \sqrt{1/2})^2 \approx 0.0858$ is reached for a sawtooth shape such that $\theta = \pm \arcsin(1/(1 + \sqrt{2}))^{1/2} \approx 40.06^\circ$.

3.2. Optimal shapes

The optimal shapes found numerically by maximising the efficiency at constant Sp are shown in figure 2. As the value of Sp is increased, the calculated shapes do converge toward Lighthill's sawtooth function. For finite values of Sp however, the singular points in $x = \lambda/4$ and $3\lambda/4$ are smoothed out.

The efficiencies of these optimal shapes are shown in figure 3 as a function of the Sperm number. We see that the efficiency is a monotonically increasing function of Sp , which reveals, as expected, that an increase of the bending rigidity leads to an increase of the internal energetic cost. The external energetic cost, or the energy given to the fluid, is quantified in this figure by also plotting the efficiency η_{fluid} using (2.9) but with P equal to the rate of dissipation in the fluid alone. The ratio between η and η_{fluid} corresponds to

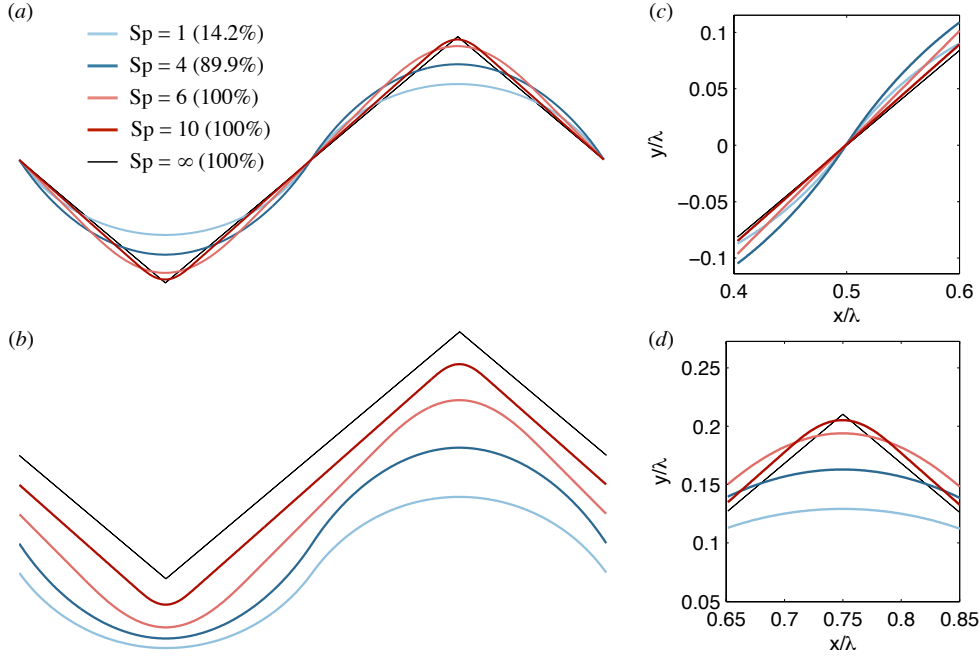


FIGURE 2. Energetically-optimal flagellum shapes for different Sperm numbers, Sp . The saw-tooth function, with an angle of $\pm 40.06^\circ$, is the solution of Lighthill (1975) and corresponds to an infinite Sperm number (thin black line). The percentages in (a) refer to the proportion of the power expended by the internal motors (torques) which ends up dissipated in the viscous fluid (see also inset of figure 3). In (a) and (b) we display the overall shapes over a single wavelengths, both superimposed (a) and shifted (b). In (c) we zoom in on the part of the flagellum which intersects its swimming axis and in (d) we show a zoom of the region with largest curvature.

the ratio between the power given to the fluid and the total power spent and is plotted as an inset in the figure (that ratio is also reported for the five optimal shapes in figure 2). When $Sp \lesssim 2.7$, more than half of the power is spent internally whereas when $Sp \gtrsim 5$, the power spent internally is almost negligible (although the optimal shapes continue to depend on the value of Sp).

In figure 4, the angle and curvature of the optimal shapes are analysed as Sp is varied. First, it appears that the maximum curvature of the shape (located in $x = \lambda/4$ and $3\lambda/4$) is an increasing function of the Sperm number. As anticipated, increasing the bending rigidity yields a smoother shape. As illustrated in figure 4c however, this monotonic increase of the maximum curvature corresponds to qualitatively different distributions of the curvature along the flagellum length. For small Sp , the curvature is almost constant on the intervals $0 < x < \lambda/2$ and $\lambda/2 < x < \lambda$ with an abrupt jump (change of sign) at $x = \lambda/2$. In that limit, the flagellum shape is an assembly of arcs of circles with identical radii. For $1 \lesssim Sp \lesssim 5$, the curvature is no longer constant on the half-wavelengths, but there is still a jump of curvatures in $x = \lambda/2$. Finally, for $Sp \gtrsim 5$, the jumps disappear and the curvature is zero in two intervals centred around $x = 0$ and $\lambda/2$; in this limit of large Sp , the region of non-zero curvature is concentrated in small intervals around $x = \lambda/4$ and $3\lambda/4$, the extent of these region decreasing as Sp increases. These different regimes are also apparent in figure 4b when looking at the maximum angle θ_{\max} between the flagellum centreline and the swimming direction (see also the zoom on the shapes in figure 2c). For small values of the Sperm number ($Sp \lesssim 3.4$), this midpoint angle increases

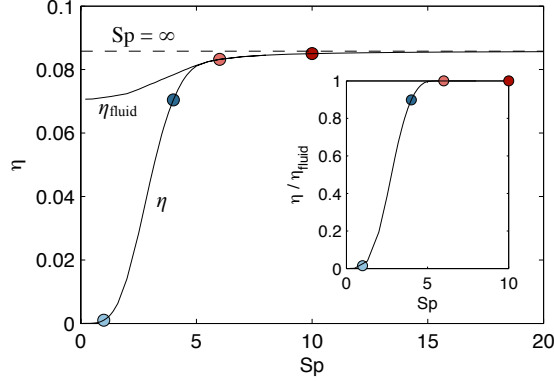


FIGURE 3. Efficiency, η , of the optimal flagellum shape as a function of the Sperm number (line with circles). The coloured symbols correspond to the cases from figure 2. The additional solid line shows the efficiency η_{fluid} calculated by considering only the fluid power while the dashed line shows the solution of Lighthill (1975), $\eta_{\text{fluid}} = (1 - \sqrt{1/2})^2 \approx 0.0858$, corresponding to an infinite Sperm number. Inset: proportion of the total internal power dissipated in the surrounding fluid.

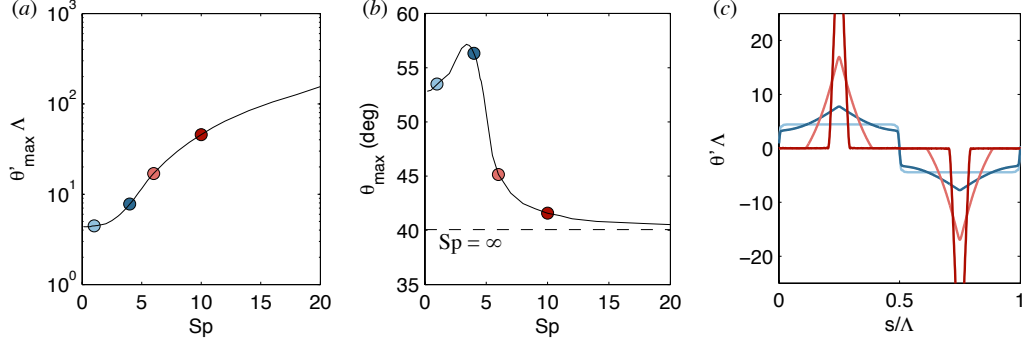


FIGURE 4. Curvature and maximum angle of the optimal solutions. (a): Maximum curvature (normalised by λ) as a function of Sp . (b) Maximum angle (in degrees), located at $x = \lambda/2$, as a function of Sp . (c) Distribution of dimensionless curvature along the flagellum axis, x , for $Sp = 1, 4, 6$, and 10 (same colour code as in the other figures).

with Sp to reach a local maximum of roughly 57° , followed by a decrease toward the value of 40.06° predicted by Lighthill (1975) corresponding to an infinite Sperm number.

4. Discussion

In this paper, we have computed the energetically-optimal shape of a flagellum deforming as a pure travelling wave. When the energetic cost is defined as the irreversible power expended by the internal molecular motors actuating the flagellum, this optimisation calculation yields a family of shapes parametrised by a single dimensionless number, the Sperm number, which quantifies the ratio between viscous and elastic effects. When the Sperm number is asymptotically small, the optimal shape is found to be an assembly of circular arcs of constant absolute curvatures. When it is asymptotically large, the optimal shape tends to the sawtooth shape found by Lighthill (1975) by considering only the power dissipated in the fluid.

At this point, two comparisons with past work should be made. First, the calculated shapes can be compared with the results of past optimisation studies. Specifically, we

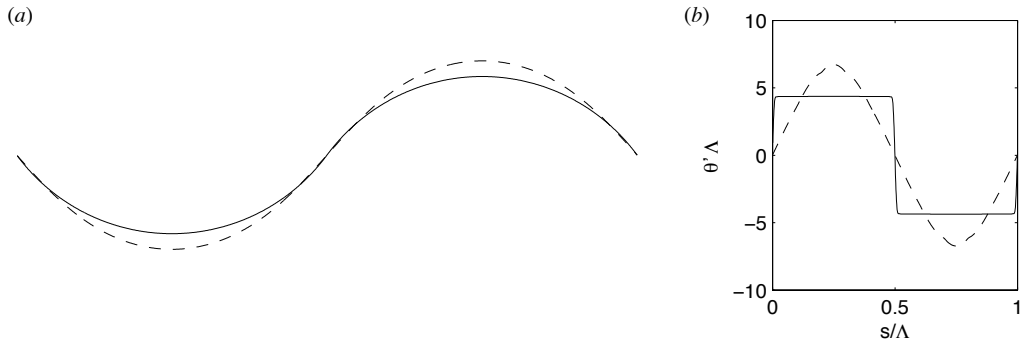


FIGURE 5. Comparison between the optimal flagellum shape obtained in the present model (solid line) and the one obtained by Spagnolie & Lauga (2010) (dashed line) in the elastic regime (i.e. $Sp \ll 1$): (a) waveforms; (b) distribution of curvatures.

look back at the study of Spagnolie & Lauga (2010) who proposed a physical regularisation of Lighthill’s shape by replacing, in (2.9), the rate of viscous dissipation in the fluid by a linear combination of that dissipation rate and the bending energy stored elastically in the flagellum per period. In the limit of strong elastic cost, or equivalently in the asymptotic limit of vanishing Sperm number, our results are compared to the ones of Spagnolie & Lauga (2010) by juxtaposing the optimal waveforms (figure 5a) and the corresponding distribution of curvatures (figure 5b). The optimal shape obtained in the present work for vanishing Sperm number is composed of circular arcs with constant curvature alternating in sign, and has an hydrodynamic efficiency $\eta_{\text{fluid}} \approx 7.1\%$. In contrast, the optimal shape in Spagnolie & Lauga (2010), which is also smooth, is characterised by a sinusoidally-varying shape angle $\theta(s)$ (and thus a sinusoidally-varying curvature) with a smaller hydrodynamic efficiency of $\eta_{\text{fluid}} \approx 6.1\%$. The crucial difference in the analysis between the two studies is that the work of Spagnolie & Lauga (2010) penalises all curvature along the flagellum equally through the use of the bending energy measuring the mean square curvature along the shape. As a difference, the present study only penalises location along the flagellum where irreversible work is being done.

A second comparison can be made with the shapes of actual biological organisms. This can be done both qualitatively and quantitatively. In a famous 50-year-old study, Brokaw & Wright (1963) described in detail the flagellar waveform of *Ceratium*, a marine dinoflagellate, and reported that contrary to common knowledge “the regular form of the wave is not sinusoidal” but the bent regions are “circular arcs in which the curvature is constant throughout the bend”. In a followup work analysing the shapes of spermatozoa of marine invertebrates, Brokaw (1965) similarly found that the observed shapes “contain regions of constant bending, forming circular arcs, separated by shorter unbent regions”. These results indicate that the optimal shapes found in the present study for small Sp , which exhibit constant curvature, agree qualitatively with those observed experimentally.

From a quantitative standpoint, we can further compare the results of the present work with experimental measurements of five flagellar shapes of spermatozoa (*Chaetopterus*, *Ciona*, *Colobocentrotus*, *Lytechinus*, *Psammechinus*), and one eukaryotic cell (*Tripanosoma cruzi*), all displaying two-dimensional flagellar beat (Table 1), and whose characteristics have been reported in Brennen & Winnet (1977), Brokaw (1965), and Gray & Hancock (1955). Averaging over all six species, the typical ratio between the flagellar wave amplitude and wavelength is found to be $h/\lambda \approx 0.165$, while the typical maximum curvature is $\theta'_{\text{max}} \approx 5.75/\Lambda$. Lighthill’s optimal shape gives $h/\lambda \approx 0.209$ and $\theta'_{\text{max}} = \infty$. By contrast, in our optimal calculation for $Sp = 4$, the optimal shapes are

		λ	h	h/λ	$\theta'_{\max}\Lambda$
EXPERIMENTS	annelid (<i>Chaetopterus</i>)	19.5 μm	3.8 μm	0.194	5.93
	tunicate (<i>Ciona</i>)	22 μm	4.3 μm	0.195	5.45
	sea urchin (<i>Colobocentrotus</i>)	30 μm	2.8 μm	0.093	—
	sea urchin (<i>Lytechinus</i>)	22.6 μm	4.6 μm	0.203	5.86
	sea urchin (<i>Psammechinus</i>)	24 μm	4.0 μm	0.166	—
	protist (<i>Trypanosoma cruzi</i>)	3.5 μm	0.5 μm	0.142	—
MODELS	present model (Sp = 1)	0.856 Λ	0.110 Λ	0.128	4.45
	present model (Sp = 4)	0.806 Λ	0.131 Λ	0.163	7.75
	present model (Sp = 6)	0.774 Λ	0.150 Λ	0.194	16.9
	present model (Sp = 10)	0.768 Λ	0.158 Λ	0.205	45.7
	Lighthill's model (Sp = ∞)	0.766 Λ	0.161 Λ	0.209	∞

TABLE 1. Comparison of the wavelength, λ , amplitude, h , amplitude-to-wavelength ratio, h/λ , and the maximum dimensionless curvature, $\theta'_{\max}\Lambda$ (when available), of five spermatozoa flagellar shapes and one protist displaying two-dimensional beating (data from Brennen & Winnet 1977; Brokaw 1965; Gray & Hancock 1955), with the results of the present model and Lighthill's optimal shape.

characterised by $h/\lambda \approx 0.163$ and $\theta'_{\max} = 7.75/\Lambda$, while for Sp = 1, we obtain shapes with $h/\lambda \approx 0.128$ and $\theta'_{\max} = 4.45/\Lambda$. What is the value of Sp that should be used for comparison? For spermatozoa, the bending rigidity of the axoneme is believed to be of the order of $B \approx 2.5 \times 10^{-23} - 4.4 \times 10^{-22} \text{ N m}^2$ (Hines & Blum 1983; Gittes *et al.* 1993; Camalet *et al.* 1999), the typical period $T \approx 0.04 \text{ s}$ (Brokaw 1965), and the drag coefficient $\xi_{\perp} \approx 0.003 \text{ Pa s}$ in water (assuming an aspect ratio $\Lambda/a = 200$, with a the radius of the flagellum, Lighthill 1975). Using equation (2.10), the value of the persistence length is therefore $\ell \approx 4 - 9 \mu\text{m}$. Since $\Lambda \approx 28 \mu\text{m}$ on average for the spermatozoa reported in Table 1, the Sperm number of a typical spermatozoon is $\text{Sp} = \Lambda/\ell \approx 3 - 7$. Our optimization approach is therefore able to generate shapes which are close to the experimental observations, suggesting that perhaps eukaryotic flagella are indeed mechanically optimal.

We thank Mario Sandoval for his help gathering the data in Table 1. We acknowledge supports from the European Union (fellowship PIOF-GA-2009-252542 to C.E.) and the US National Science Foundation (grant CBET-0746285 to E.L.).

REFERENCES

- ALBERTS, B., JOHNSON, A., LEWIS, J., RAFF, M., ROBERTS, K. & WALTER, P. 2007 *Molecular Biology of the Cell*, 5th edition. Garland Science, NY.
- ALEXANDER, R. MCN. 1992 A model of bipedal locomotion on compliant legs. *Phil. Trans. R. Soc. Lond. B* **338**, 189–198.
- ALOUGES, F., DESIMONE, A. & LEFEBVRE, A. 2008 Optimal strokes for low Reynolds number swimmers: An example. *J. Nonlinear Science* **18** (3), 277–302.
- AUDOLY, B. & POMEAU, Y. 2010 *Elasticity and geometry*. Oxford University Press.
- AVRON, J. E. & RAZ, O. 2008 A geometric theory of swimming: Purcell's swimmer and its symmetrized cousin. *New J. Phys.* **10**, 063016.
- BRAY, D. 2000 *Cell Movements*. New York, NY: Garland Publishing.
- BRENNEN, C. & WINNET, H. 1977 Fluid mechanics of propulsion by cilia and flagella. *Ann. Rev. Fluid Mech.* **9**, 339–398.
- BROKAW, C. J. 1965 Non-sinusoidal bending waves of sperm flagella. *J. Exp. Biol.* **43**, 155.

- BROKAW, C. J. & WRIGHT, L. 1963 Bending waves of the posterior flagellum of *Cerratum*. *Science* **142**, 1169–1170.
- CAMALET, S., JULICHER, F. & PROST, J. 1999 Self-organized beating and swimming of internally driven filaments. *Phys. Rev. Lett.* **82**, 1590–1593.
- CHILDRESS, S. 1981 *Mechanics of Swimming and Flying*. Cambridge: Cambridge University Press.
- COX, R. G. 1970 The motion of long slender bodies in a viscous fluid. Part 1. General theory. *J. Fluid Mech.* **44**, 791–810.
- ELOY, C. & LAUGA, E. 2012 Kinematics of the most efficient cilium. *Phys. Rev. Lett.* **109**, 038101.
- FUJITA, T. & KAWAI, T. 2001 Optimum shape of a flagellated microorganism. *JSME Int. J. Ser. C* **44**, 952–957.
- GITTES, F., MICKEY, B., NETTLETON, J. & HOWARD, J. 1993 Flexural rigidity of microtubules and actin-filaments measured from thermal fluctuations in shape. *J. Cell Biol.* **120**, 923–934.
- GRAY, J. & HANCOCK, G. J. 1955 The propulsion of sea-urchin spermatozoa. *J. Exp. Biol.* **32**, 802–814.
- HIGDON, J. J. L. 1979a Hydrodynamic analysis of flagellar propulsion. *J. Fluid Mech.* **90**, 685–711.
- HIGDON, J. J. L. 1979b Hydrodynamics of flagellar propulsion—Helical waves. *J. Fluid Mech.* **94**, 331–351.
- HINES, M. & BLUM, J. J. 1983 Three-dimensional mechanics of eukaryotic flagella. *Biophys. J.* **41**, 67–79.
- LAUGA, E. 2011 Life around the scallop theorem. *Soft Matter* **7**, 3060 – 3065.
- LAUGA, E. & POWERS, T. R. 2009 The hydrodynamics of swimming microorganisms. *Rep. Prog. Phys.* **72**, 096601.
- LESHANSKY, A. M., KENNETH, O., GAT, O. & AVRON, J. E. 2007 A frictionless microswimmer. *New J. Phys.* **9**, 126.
- LIGHTHILL, J. 1975 *Mathematical Biofluidynamics*. SIAM, Philadelphia.
- MICHELIN, S. & LAUGA, E. 2010 Efficiency optimization and symmetry-breaking in an envelope model for ciliary locomotion. *Phys. Fluids* **22**, 111901.
- MICHELIN, S. & LAUGA, E. 2011 Optimal feeding is optimal swimming for all pécelet numbers. *Phys. Fluids* **23**, 101901.
- MICHELIN, S. & LAUGA, E. 2013 Unsteady feeding and optimal strokes of model ciliates. *J. Fluid Mech.* **715**, 1–31.
- OSTERMAN, N. & VILFAN, A. 2011 Finding the ciliary beating pattern with optimal efficiency. *Proc. Nat. Acad. Sc. USA* **108**, 15727–15732.
- PIRONNEAU, O. & KATZ, D. F. 1974 Optimal swimming of flagellated micro-organisms. *J. Fluid Mech.* **66**, 391.
- PIRONNEAU, O. & KATZ, D. F. 1975 Optimal swimming of motion of flagella. In *Swimming and Flying in Nature* (ed. T.Y. Wu, C.J. Brokaw & C Brennen), , vol. 1, pp. 161–172. New-York: Plenum.
- PURCELL, E. M. 1977 Life at low Reynolds number. *Am. J. Phys.* **45**, 3.
- SHAPER, A. & WILCZEK, F. 1987 Self-propulsion at low Reynolds number. *Phys. Rev. Lett.* **58**, 2051–2054.
- SHAPER, A. & WILCZEK, F. 1989a Efficiencies of self-propulsion at low Reynolds number. *J. Fluid Mech.* **198**, 587–599.
- SHAPER, A. & WILCZEK, F. 1989b Geometry of self-propulsion at low Reynolds number. *J. Fluid Mech.* **198**, 557–585.
- SPAGNOLIE, S. E. & LAUGA, E. 2010 The optimal elastic flagellum. *Physics of Fluids* **22**, 031901.
- SPAGNOLIE, S. E. & LAUGA, E. 2011 Comparative hydrodynamics of bacterial polymorphism. *Phys. Rev. Lett.* **106**, 058103.
- TAM, D. & HOSOI, A. E. 2007 Optimal stroke patterns for purcell’s three-link swimmer. *Phys. Rev. Lett.* **98**, 068105.